The influence of an alkenyl terminal group on the mesomorphic behaviour and electro-optic properties of fluorinated terphenyl liquid crystals†

Julita S. Gasowska,[a] Stephen J. Cowling,[a] Martin C. R. Cockett,[a] Michael Hird,[b] Robert A. Lewis,[b] E. Peter Raynes[c] and John W. Goodby[*a]

Novel liquid crystal terphenyls with two, three and four lateral fluoro substituents and an alkene unit at the end of a terminal chain are presented in terms of synthesis, mesomorphic behaviour and electro-optic properties. The difluoro analogues were found to exhibit the smectic C phase over a wide temperature range, with short temperature ranges of the smectic A and the nematic phase above. Very low melting points were recorded for the trifluoro analogues, and the shorter chain homologues of these materials exhibit the nematic phase over a wide temperatures with a monotropic smectic C phase and the higher homologues exhibit the smectic C phase over a wide temperature range with the nematic phase above. The tetrafluoroterphenyls exhibit the nematic phase over a wide temperature range with the complete absence of smectic phases. As appropriate, the materials were evaluated for dielectric anisotropy and threshold voltage in nematic phase, and mixed with a chiral dopant to evaluate the spontaneous polarisation, tilt angle and switching times in the chiral smectic C phase. The results show that these compounds are strong potential candidates for application in both vertically aligned nematic (VAN) and ferroelectric liquid crystal (FLC) devices.

1. Introduction

Over the last decade liquid crystal displays (LCDs) have become the standard technology for mobile phones, PC monitors and televisions. Practically all of these devices are based on nematic liquid crystals, however, the switching time of milliseconds is still an issue for video applications. With future LCD TVs projected to become more complex, possibly moving from 2D to 3D images and with the refresh rates moving towards the 200 Hz range, Souk of Samsung challenged the international scientific community at the International Liquid Crystal Conference in Korea[1] to develop faster LC switching modes.

One of the more common LCD modes in usage today is the vertically aligned nematic (VAN) cell which utilises materials with negative dielectric anisotropy.[2–5] Response times are closely related to the magnitude of the dielectric anisotropy, the higher the negativity the better, and the lower the viscosity the better. Such requirements dictate the design and synthesis of materials with molecular structures of a cylindrical shape that possess large lateral dipoles. In this article we describe the synthesis and properties of di-, tri- and tetra-fluorinated terphenyls

(see structure **III**), which are cylindrical in shape, and we show through dielectric studies that the fluoro substituents can couple to give relatively large values of the negative dielectric anisotropy.
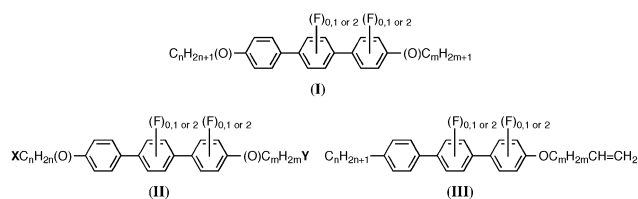
An alternative approach to addressing the issue of response time is to deploy a different type of liquid crystal phase. For example, because of the coupling between the electric field and the permanent polarisation, surface-stabilised ferroelectric liquid crystal displays (SSFLCDs) offer switching times in the microsecond regime, one hundred to one thousand times faster than nematic switching modes. In combination with silicon back planes, such devices have already been used in projection applications and spatial light modulators.[6]

Thus in this article we also report on the development of novel ferroelectric liquid crystals and their potential for use in fast, high-resolution, low-voltage ferroelectric liquid crystal on silicon (LCOS) devices with optimised performance. Such light processors can be used in amplitude modulation or phase modulation mode. With amplitude modulation, very high-resolution professional monitors and near-to-eye 3D imaging can be achieved. Compared to digital mirror devices, ferroelectric liquid crystal devices can have considerably higher pixel density, leading to more pixels on the same chip area and cost

[a]Department of Chemistry, University of York, Heslington, York, UK YO10 5DD. E-mail: jwg500@york.ac.uk; sc520@york.ac.uk
[b]Department of Chemistry, University of Hull, Cottingham Road, Hull, UK HU6 7RX. E-mail: m.hird@hull.ac.uk; r.a.lewis@hull.ac.uk
[c]Department of Engineering, University of Oxford, Parks Road, Oxford, UK OX1 3PJ. E-mail: peter.raynes@eng.ox.ac.uk

† Electronic supplementary information (ESI) available: Full synthetic details for the preparation of compounds **5–25** are given along with full description of characterisation and evaluation techniques. See DOI: 10.1039/b914260f

effectiveness for high pixel numbers. Due to the fast switching speed of ferroelectric liquid crystals, colour images can be realised with one single ferroelectric device using sequential colour illumination.

The basic molecular design of ferroelectric host and dopant liquid crystals usually involves the incorporation of a central aromatic or heterocyclic core unit which is sandwiched between two terminal aliphatic chains.[7] In this case fluoro-substituted terphenyls (see structure **I**) have also shown considerable promise in ferroelectric systems for which response times have been achieved in the 10 to 100 microsecond (μs) regime.[8,9] Typically, when molecules with this type of architecture self-organise they do so with their rigid, aromatic parts tending to pack together and their flexible/dynamic aliphatic chains orienting together. Thereby the overall system becomes locally microphase segregated. Consequently, the main target of material design has been, by default, the variation in the structure of the central core region of the molecules, *e.g.*, changing the number and location of fluoro substituents, in the belief that the core is more important in influencing mesophase incidence, mesophase temperature range, isotropization point, melting point, mesophase sequence, and the reorientational viscosity associated with the mesophase. However, few systematic studies have been reported where the terminal positions of the aliphatic chains have been manipulated, *e.g.*, **X** and **Y** in structure **II** for fluoroterphenyls. Through these limited, and unsystematic, studies there has been a realisation that small changes to the termini of the molecular structure can have a very marked effect on liquid crystal phase formation and related physical properties, particularly for ferroelectric phases.

Therefore, understanding the interactions at, and between, the interfaces of the layers in lamellar smectic phases is of practical importance in the development of ferroelectric devices and displays. There are a number of interactions to consider in devices which include the liquid crystal surface interactions, the penetration of the surface interactions into the bulk of the liquid crystal phase, the strength of the lateral interactions between the molecules, and the strength of the interactions between the layers, as shown in Fig. 1. The strength of the surface interactions controls the surface anchoring energies and hence the bistability of the device operation. The strength of the interactions between the layers controls the shape of the hysteresis loop for the ferroelectric phase. Weak interlayer (out-of-plane) interactions can lead to a collapse of the hysteresis loop, and hence these

can markedly affect device configuration, construction and performance.[10] For example, weak interlayer interactions leading to the collapse of the hysteresis loop result in a linear electro-optic response to an applied electric field (V-shaped switching), thereby enabling the device to exhibit a grey-scale response suitable for video-frame rate applications.

Overall, in a situation where there is a need to design materials with molecular structures that will induce selective mesophase formation, being able to control mesophase structure simply by terminal group selection is a powerful weapon. Thus, the wider aims of our research are to develop a wide range of materials based on structure **II**, in particular where the terminal groups **X** or **Y** are silanes, siloxanes, ethers and fluorocarbons. In this article we examine the intermediary alkenic terminal systems, which ultimately can be further derivatised through, for example, hydrosilylation, to give other liquid crystal systems possessing terminal microphase segregating groups that exhibit stronger interactions. Thus, in this article we focus on alkenic materials based on structure **III**, which are similar to the alkanes, in order to compare the uses of the same family of materials in VAN-LCD and SSFLCD modes of operation.

2. Experimental

Confirmation of the structures of intermediates and products was obtained by ^{1}H and ^{13}C NMR spectroscopy (JEOL ECX 400 MHz), infrared spectroscopy (Shimadzu IRPrestige-21 Fourier transform infrared spectrophotometer) and mass spectrometry (EI-MS, AUTOSPEC WATERS-MICROMASS). The purity of the compounds in Tables 1–3 was checked by HPLC (Shimadzu Prominence LC-20AT) and all compounds were >99.9% pure.

General synthetic pathway to the ω-alkenic materials is shown in Schemes 1 and 2. Full synthetic details are given in the ESI.†

Compounds **1a**, **1b** and **2** (Scheme 1) were prepared using synthetic methods which have been previously published.[11] Compounds **3a** and **3b** were prepared using a Suzuki coupling reaction and they were subsequently lithiated using *n*-butyl-lithium and converted into the boronic acid with trimethyl borate. The boronic acids were oxidised using hydrogen peroxide to give phenols **4a** and **4b** in good yields. A Williamson etherification using potassium carbonate and the appropriate ω-bromoalkene yielded alkenic difluoroterphenyls **5–8**. A Suzuki coupling reaction between compounds **9** and **10** and between compounds **12** and **13** gave terphenyl compounds **14a**, **14b**, **15a** and **15b** in excellent yields. These compounds were converted into boronic acids and oxidised to the phenol compounds **16a**, **16b**, **17a** and **17b** in the same way as for the preparation of compounds **4a** and **4b**. A Williamson etherification using potassium carbonate and the appropriate ω-bromoalkene gave tri- and tetrafluoroterphenyls **18–25**. All the final compounds were purified by column chromatography and recrystallisation.

2.1. Evaluation of structural and physical properties

Detailed descriptions of the evaluation and characterisation techniques for the determination of transition temperatures, physical properties and structure analysis are provided in the ESI†.
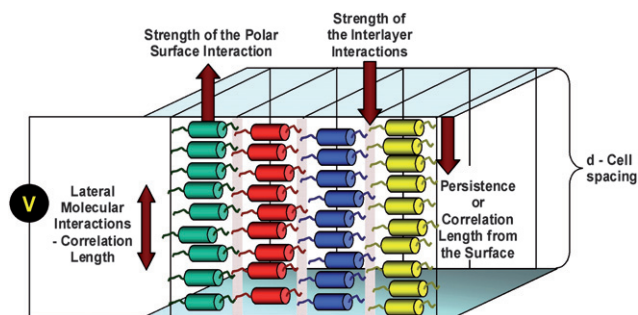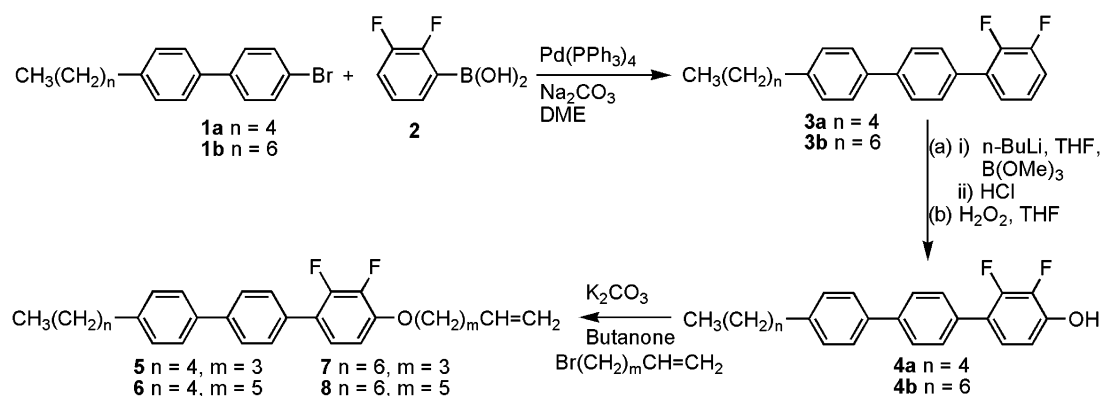

Fig. 1 A typical device arrangement for smectic liquid crystals, with the layer planes perpendicular to the cell surface. The important intermolecular and surface interactions are shown.

Scheme 1 General synthetic route for the preparation of alkenic difluoroterphenyls **5–8**.

3. Results and discussion

### 3.1. Mesophase classification and melting behaviour

The results obtained on the melting behaviour of all of the compounds are compiled together in Tables 1–3, where Table 1 collects the family of materials possessing two fluoro substituents, Table 2 three fluoro substituents, and Table 3 four fluoro substituents. The transition temperatures reported were determined by thermal polarised light optical microscopy, whereas the melting points and recrystallisation temperatures were determined by differential scanning calorimetry.

The mesophases were characterised from their natural and paramorphotic defect textures as described by Gray and Goodby.[12] The difluoroterphenyls (Table 1) characteristically exhibit nematic, smectic A and smectic C phases, where the smectic A to smectic C phase transition is essentially second order and the smectic A temperature range is relatively short.
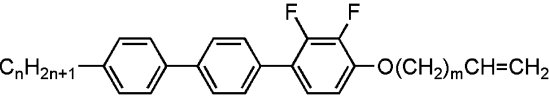
Coupled with a N–A–C phase sequence makes them ideal candidates as host materials in ferroelectric smectic C* mixtures for applications in surface stabilised ferroelectric liquid crystal displays, SSFLCDs.

In contrast to the difluoroterphenyls, the trifluoroterphenyl analogues (Table 2) show very low melting points, and they possess less smectic character, with the smectic A phase being suppressed. Thus the trifluoroterphenyls exhibit just nematic and smectic C phases, with the latter phase being monotropic for the shorter chain homologues. Hence the compounds could make useful components in mixtures for both VAN and FLC applications.
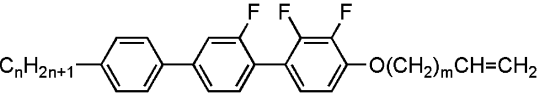
The tetrafluoroterphenyls (Table 3) show that the inclusion of an extra fluoro substituent completely suppresses the formation of smectic phases, and thus the compounds are nematogens melting around 60 °C and clearing around 100 °C. From the point of view of mesomorphic properties these materials are
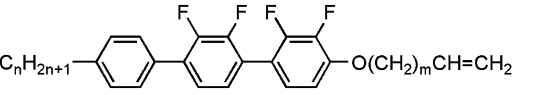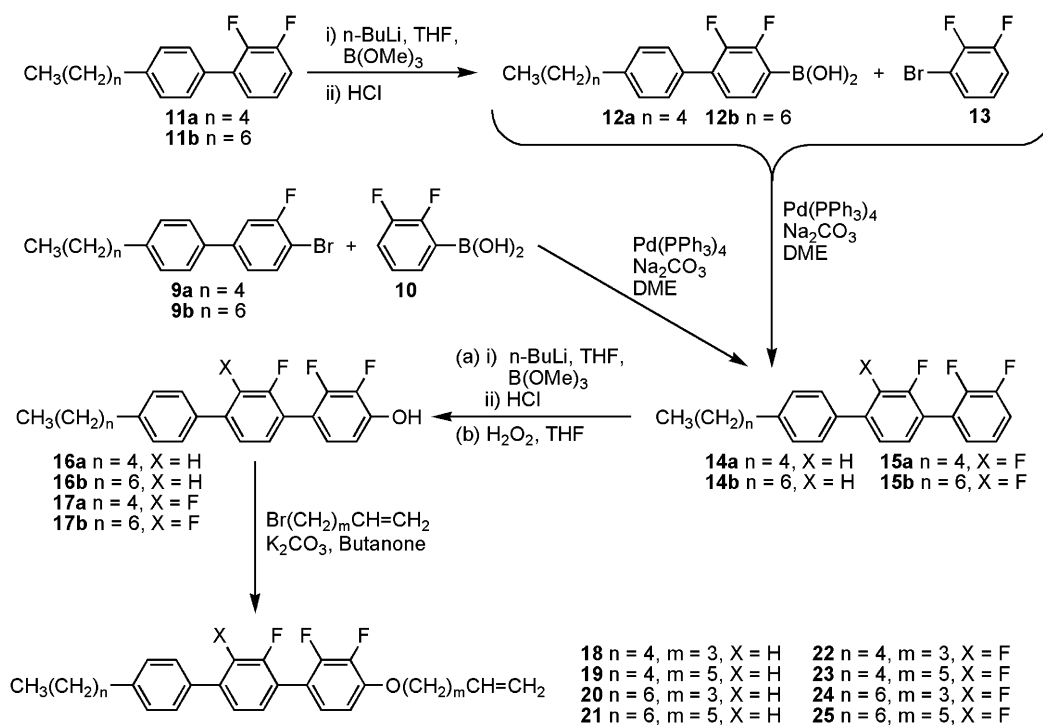

Scheme 2 General synthetic route for the preparation of alkenic tri- and tetrafluoroterphenyls **18–25**.

Table 1 Phase classification, transition temperatures (°C) and enthalpies of transition [ΔH, J g⁻¹] for compounds **5–8**
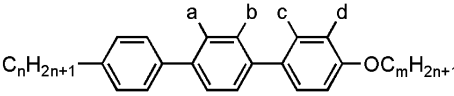
C_nH_{2n+1}—⟨⟩—⟨⟩—⟨F F⟩—O(CH₂)_mCH=CH₂

Cpd no.	n	m	Cr		SmC		SmA		N		Iso Liq
5	5	3	•	101.31 [29.91]	•	139.37 [0.26]	•	151.95 [5.35]	•	169.41 [5.57]	•
6	5	5	•	89.87 [26.01]	•	136.85 [0.20]	•	146.37 [4.41]	•	159.94 [5.36]	•
7	7	3	•	97.53 [23.27]	•	140.48 [0.14]	•	157.76 [7.62]	•	162.80 [4.89]	•
8	7	5	•	87.24 [23.65]	•	141.71 [0.23]	•	152.18 [5.54]	•	155.27 [5.02]	•

Table 2 Phase classification, transition temperatures (°C) and enthalpies of transition [ΔH, J g⁻¹] for compounds **18–21**[a]

C_nH_{2n+1}—⟨⟩—⟨F⟩—⟨F F⟩—O(CH₂)_mCH=CH₂

Cpd no.	n	m	Cr		SmC			N		Iso Liq
18	5	3	•	48.44 [44.67]	(•	35.90) [0.99]	•	117.06 [1.48]	•
19	5	5	•	46.09 [51.43]	(•	36.29) [0.71]	•	109.42 [1.50]	•
20	7	3	•	30.39 [32.71]	•	69.95 [0.50]	•	111.38 [2.80]	•
21	7	5	•	28.15 [40.95]	•	71.18 [1.03]	•	107.02 [3.15]	•

[a] Values in parenthesis represent a monotropic transition.

Table 3 Phase classification, transition temperatures (°C) and enthalpies of transition [ΔH, J g⁻¹] for compounds **22–25**

C_nH_{2n+1}—⟨⟩—⟨F F⟩—⟨F F⟩—O(CH₂)_mCH=CH₂

Cpd no.	n	m	Cr		N		Iso Liq
22	5	3	•	56.90 [57.63]	•	108.78 [1.54]	•
23	5	5	•	63.76 [53.84]	•	101.08 [1.16]	•
24	7	3	•	53.05 [37.20]	•	103.08 [2.11]	•
25	7	5	•	64.84 [56.38]	•	97.06 [1.95]	•

Table 4 Phase classification and transition temperatures (°C) of difluoro-, trifluoro- and tetrafluoroterphenyl n-alkyl analogues[a]

C_nH_{2n+1}—⟨⟩—⟨a b⟩—⟨c d⟩—OC_mH_{2m+1}

n	m	a	b	c	d	Transition temperatures/°C
5	6	H	H	F	F	Cr 97.5 SmC 145.5 N 166.0 Iso liq[13]
5	8	H	H	F	F	Cr 93.5 SmC 144.0 SmA 148.0 N 159.0 Iso liq[13]
7	8	H	H	F	F	Cr 89.5 SmC 148.0 SmA 151.5 N 154.0 Iso liq[13]
5	6	H	F	F	F	Cr 43.8 (SmC 38.1) N 112.3 Iso liq[11]
5	8	H	F	F	F	Cr 47.3 SmC 50.2 N 110.3 Iso liq[11]
7	6	H	F	F	F	Cr 40.1 SmC 75.7 N 111.8 Iso liq[11]
7	8	H	F	F	F	Cr 48.0 SmC 81.0 N 108.8 Iso liq[11]
5	6	F	F	F	F	Cr 61.1 N 107.5 Iso liq[11]
7	6	F	F	F	F	Cr 55.1 (SmC 50.7) N 103.1 Iso liq[11]

[a] Values in parenthesis represent a monotropic phase transition.

potentially suitable for applications in vertically aligned nematic liquid crystal displays, VAN-LCDs.

Comparisons, in terms of transition temperatures and mesophase morphology, can be made with the standard alkyl chain analogues shown in Table 4. It can be seen that the transition sequences are almost identical, and that the transition temperatures are very similar for homologues with similar aliphatic chain lengths. Thus in this case the incorporation of an alkenic unit at the terminus of the alkoxy chain has little effect on mesophase/melting behaviour.

3.2. Electrical field studies

3.2.1. Nematic phases under applied electrical fields. Several materials were investigated in the nematic phase under applied electric fields. As the difluoro-substituted materials tended to show strong smectic properties they were not investigated for physical properties in the nematic phase. Moreover as they exhibited relatively short temperature range nematic phases, comparisons across the three series of compounds would be meaningless. Thus attention was focused on the electrical field behaviour of the tri- and tetrafluoroterphenyls. In the following we describe a direct comparison between compounds **18** and **22**, comparison between other pairs of homologues were, however, found to be similar. Fig. 2 shows the switching behaviour of the nematic phase of compound **18** as a function of the reduced temperature. Fig. 2a shows the values of the parallel dielectric permittivity, $\varepsilon_{\parallel}$, and the perpendicular dielectric permittivity, $\varepsilon_{\perp}$, as a function of the reduced temperature from the clearing point. Similarly, Fig. 2b shows the values on heating and cooling of the dielectric anisotropy, $\Delta\varepsilon$, and Fig. 2c shows the threshold voltage for switching, both as a function of the reduced temperature from the clearing point. Fig. 2a shows that both permittivities rise linearly with reduced temperature. At a reduced temperature of 60 °C the order parameter, S, determined via the use of Maier–Meier theory[14] was found to be 0.65, showing that the nematic phase was fairly well-ordered. The dielectric anisotropy, shown in Fig. 2b, was found to reach a value of −4.7 at 80 °C below the clearing point and just before recrystallisation. Interestingly, the
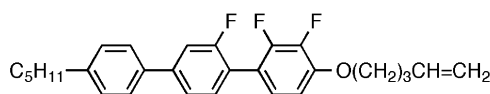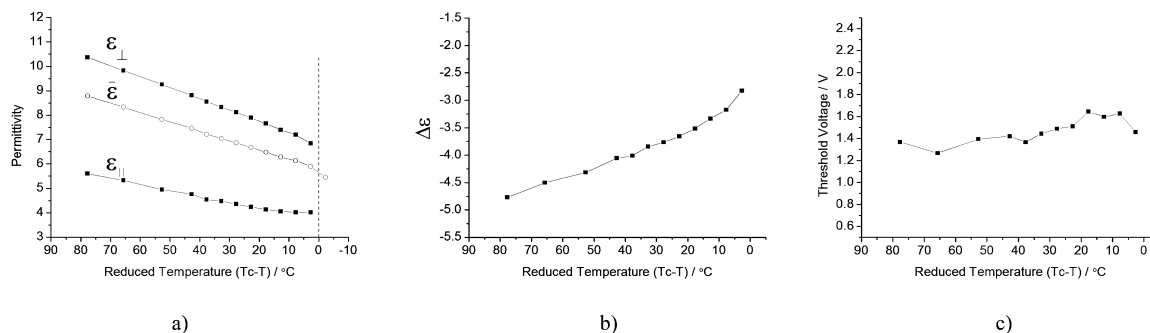
C_5H_{11} ⬡—⬡ O(CH$_2$)$_3$CH=CH$_2$

18

a)

b)

c)

Fig. 2 Switching properties of the nematic phase of compound **18** as a function of reduced temperature. (a) Measurement of the parallel permittivity, $\varepsilon_{\parallel}$, and perpendicular permittivity, $\varepsilon_{\perp}$; (b) measurement of $\Delta\varepsilon$ ($\varepsilon_{\parallel} - \varepsilon_{\perp}$); and (c) threshold voltage for switching.

threshold voltage remained low, at 1.4 V for 4.6 μm cell thickness, across the whole temperature range indicating that the increasing negativity in the dielectric anisotropy offsets the increase in the viscoelastic constants as the temperature falls.

Fig. 3 shows the comparative switching behaviour of the nematic phase of compound **22** as a function of the reduced temperature. The results obtained mirror those found for compound **18**, except that the perpendicular permittivity has a much larger value, 14 *versus* 10 at a reduced temperature of 60 °C. Concomitantly, the value of the dielectric anisotropy reaches a value of almost −7.7 at a reduced temperature of 65 °C just before recrystallisation occurs. The Maier–Meier theory predicts an order parameter S of 0.6 at this value. The more negative value of the dielectric anisotropy reduces the relative threshold voltage to approximately 0.7 V for a cell thickness of 4.6 μm. Theoretically, this value should only be approximately 25% lower for the tetrafluoro compound *i.e.*, approximately 1.2 V, due to the 50% increase in $\Delta\varepsilon$. This difference may be due to misalignment occurring on cooling or else larger differences

in the elastic constants between the trifluoro and tetrafluoro systems.

The larger negative dielectric anisotropy for compound **22** in comparison to **18** can be rationalised as follows. The inter-annular twisting about the 1-1′ carbon–carbon bond of the ter-phenyl core unit suggests that the dipole associated with fluoro substituents (one or two) located on the centre ring can oppose the dipole associated with the adjacent ring that carries two fluoro substituents, thereby minimising the overall lateral dipole. As a consequence, the opposed dipoles would reduce the value of the perpendicular permittivity. The fact that the perpendicular permittivity has a larger value for compound **22** in comparison to **18** indicates that dipolar effects of the fluoro substituents are additive rather than subtractive. Geometry optimisations conducted on a series of di-substituted tetrafluoroterphenyls and trifluoroterphenyl at the DFT/B3-lyp/def2-TZVPP and RIMP2/def2-TZVPP levels of theory suggest that the fluoro substituents preferentially lie on the same side of the molecule. The aromatic rings are not equiplanar but the fluoro substituents are close
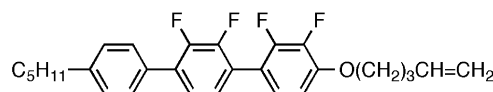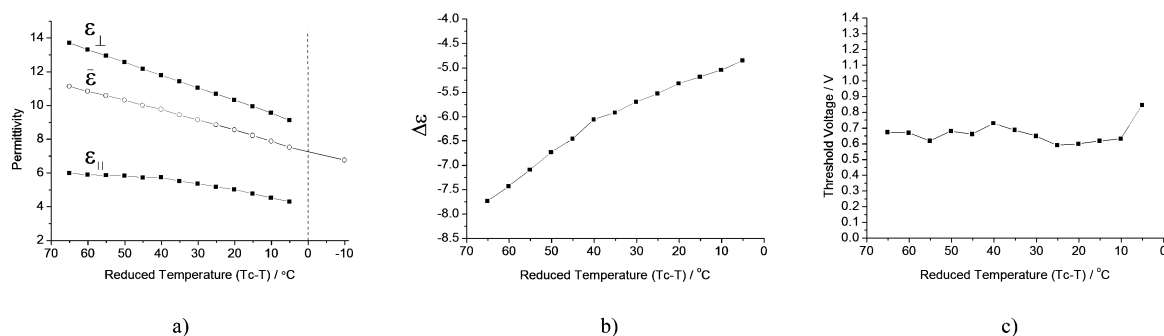
C_5H_{11} ⬡—⬡ O(CH$_2$)$_3$CH=CH$_2$

22

a)

b)

c)

Fig. 3 Switching properties of the nematic phase of compound **22** as a function of reduced temperature. (a) Measurement of the parallel permittivity, $\varepsilon_{\parallel}$, and perpendicular permittivity, $\varepsilon_{\perp}$; (b) measurement of $\Delta\varepsilon$; and (c) threshold voltage for switching.
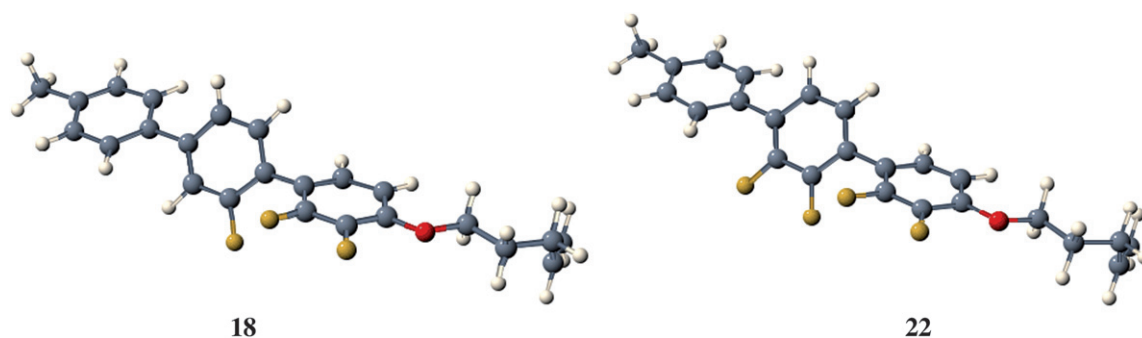
Fig. 4 Minimum energy geometries of methyl compounds related to **18** and **22** computed at the DFT/b3-lyp/def2-TZVPP level of theory.

enough to interact (see Fig. 4). For each model terphenyl, two stable conformers were identified, one in which the fluorine atoms lie on the same side of the molecule in essentially a *cis* conformation and the other in which the fluorine atoms lie on opposite sides of the molecule in a *trans* conformation. Regardless of the substituents chosen at the *ipso* position of the first ring, the *cis* conformer was consistently found to be the most stable, before and after zero point energy correction (see Table 5). At the DFT level, the difference in minimum energies varied from as low as 0.209 kJ mol⁻¹ in the methoxy-substituted tetra-fluoroterphenyl to 0.627 kJ mol⁻¹ in the methyl-substituted terphenyl. Correction for zero point energy increased these values by between 60 and 80%. For the two lighter tetra-fluoroterphenyls, optimisations were also completed at the MP2 level of theory. In both cases, this resulted in a considerable further stabilisation of the *cis* conformer compared to the *trans* with differences in minimum energies before correction for ZPE being between about 1.6 and 1.9 kJ mol⁻¹. At the DFT level, the difference in stabilities between the *cis* and *trans* conformers of compounds **18** and **22** is essentially the same with the *cis* conformer more stable by 0.23 kJ mol⁻¹ in each case (see Table 5 and Fig. 4). The results of ZPE corrected DFT calculations and MP2 calculations performed on the methyl and methoxy-substituted variants of **22** strongly suggest that the inherent stabilty of the *cis* conformers of **18** and **22** would be maintained at higher levels of theory. Thus, it appears that the preferred conformation adopted by these compounds is the result of through-space coupling between the fluoro substituents located

on adjacent rings. This observation would seem to be reinforced in the electrical field experiments, even though the molecules are in dynamic motion about their long axes in the smectic state.

3.2.2. Ferroelectric phases under applied electric fields. In order to compare the properties of the ferroelectric smectic C* phases of the materials the materials were first doped with the chiral compound BE8OF2N, structure **26**, 5 and 10% by weight,

Table 6 Phase classification and transition temperatures (°C) of BE8OF2N-doped mixtures of difluoro- and trifluoroterphenyl *n*-alkyl analogues

Cpd no.	% BE8OF2N	Transition temperatures/°C
5	5	SmC* 122.7 SmA* 146.7 N* 159.9 Iso liq
5	10	SmC* 107.3 SmA* 141.6 N* 152.1 Iso liq
6	5	SmC* 123.9 SmA* 140.5 N* 151.7 Iso liq
6	10	SmC* 106.7 SmA* 135.7 N* 144.3 Iso liq
7	5	SmC* 127.3 SmA* 152.1 N* 155.1 Iso liq
7	10	SmC* 109.5 SmA* 146.9 N* 148.0 Iso liq
8	5	SmC* 129.6 SmA* 146.1 N* 147.6 Iso liq
8	10	SmC* 118.7 SmA* 145.6 Iso liq
18	5	SmC* 60.5 N* 107.9 Iso liq
18	10	SmC* 40.1 N* 101.5 Iso liq
19	5	SmC* 48.9 N* 100.8 Iso liq
19	10	SmC* 47.5 N* 94.1 Iso liq
20	5	SmC* 64.7 SmA* 72.3 N* 104.3 Iso liq
20	10	SmC* 47.2 SmA* 73.4 N* 97.5 Iso liq
21	5	SmC* 61.8 SmA* 65.7 N* 95.5 Iso liq
21	10	SmC* 33.7 SmA* 65.5 N* 89.6 Iso liq

Table 5 DFT and MP2 absolute and zero point energy corrected minimum energies for a series of disubstituted tetrafluoroterphenyls and tri-fluoroterphenyls at the DFT/B3-lyp/def2-TZVPP and RIMP2/def2-TZVPP levels of theory

	DFT/B3-lyp/def2-TZVPP			RIMP2/def2-TZVPP		
	Cis/a.u.	*Trans*/a.u.	Δ/kJ mol⁻¹	*Cis*/a.u.	*Trans*/a.u.	Δ/kJ mol⁻¹
2,2′,3,3′-Tetrafluoro-4,4″-dimethyl-1,1′:4′,1″-terphenyl						
Energy	−1169.75899	−1169.75875	0.627	−1168.28376	−1168.28304	1.891
ZPE corrected energy	−1170.04271	−1170.04266	1.121	—	—	—
2,2′,3,3′-Tetrafluoro-4-methoxy-4″-methyl-1,1′:4′,1″-terphenyl						
Energy	−1244.96110	−1244.96102	0.209	−1243.40218	−1243.40158	1.579
ZPE corrected energy	−1244.67242	−1244.67229ᵃ	0.341	—	—	—
2,2′,3,3′-Tetrafluoro-4″-methyl-4-(pent-4-enyloxy)-1,1′:4′,1″-terphenyl						
Energy	−1400.93591	−1400.93582	0.239	—	—	—
2,2′,3-Trifluoro-4″-methyl-4-(pent-4-enyloxy)-1,1′:4′,1″-terphenyl						
Energy	−1301.69465	−1301.69456	0.231	—	—	—

ᵃ First order saddle point.

and then subjected to electrical field studies using various waveforms. Materials **22–25** were not investigated using this methodology because they do not exhibit the smectic C phase. Compounds **5–8** all exhibit N–SmA–SmC phase sequences, with second order smectic A to smectic C phase transitions. Thus typical ferroelectric behaviour was predicted for these materials. The second family of materials, **18–21**, was found to exhibit nematic to smectic C phase transitions, which were determined to be weakly first order in nature. The transition temperatures for the mixtures are shown in Table 6.
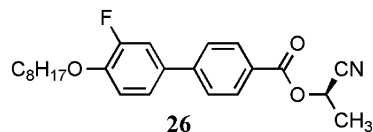
Fig. 5(a–d) shows the electrical field studies for compounds **5–8** with either 5 (a and b) or 10 wt% (c and d) of the chiral dopant **26** in cells with 4 μm spacers. The results for the tilt angle and of the spontaneous polarisation as function of the reduced temperature are compared for all of the homologues of the difluoroterphenyls.

It can be seen from the results that below a reduced temperature of 10 °C the spontaneous polarisation increases linearly, whereas the tilt angles rise at first and then level off to a value around 25°, with the homologues possessing the longer methylene chain between the terphenyl core and the alkenic group having higher values. Conversely, these homologues also have the lower spontaneous polarisations. This can be rationalised as follows: the longer methylene spacer lengths increase the relative

molecular volumes and thereby reduce the charge per unit volume, which, respectively, reduces the relative spontaneous polarisations. The longer methylene spacer chains also have the effect of inducing relatively high tilt angles, hence compounds **6** and **8** have higher tilts, but lower polarisations, even though the higher tilt angles should produce higher spontaneous polarisations. Switching studies at higher concentrations of the dopant show that the relative tilt angles are lower, whereas the spontaneous polarisations are much higher as expected.

Fig. 6(a–d) shows the results obtained for the electrical field studies of the trifluoroterphenyls. The pentyl homologues **18** and **19** exhibit monotropic nematic to smectic C phase transitions, which are at considerably lower temperatures than the enantiotropic transitions obtained for the heptyl homologues **20** and **21**. The transitions in all cases appear to be weakly first order. However, for both the 5 and the 10 wt% of the dopant the tilt angle for the pentyl homologues shows a classical first order jump at the N* to SmC* transition, whereas the heptyl homologues show second order growth in the tilt which is due to the injection of a smectic A phase in the mixtures upon addition of the chiral dopant. For both dopant concentrations the spontaneous polarisation for the heptyl homologues **20** and **21** is lower as expected in comparison to the pentyl materials **18** and **19**. Again, like the tilt angle, the spontaneous polarisation shows a first order jump at the N* to SmC* for the shorter pentyl homologues in comparison with the heptyl materials.

In addition to the evaluation of the tilt angle and the spontaneous polarisation, the response time was also determined for a number of materials. A typical example is shown in Fig. 7 for compound **8**. The response time is shown for two mixtures of
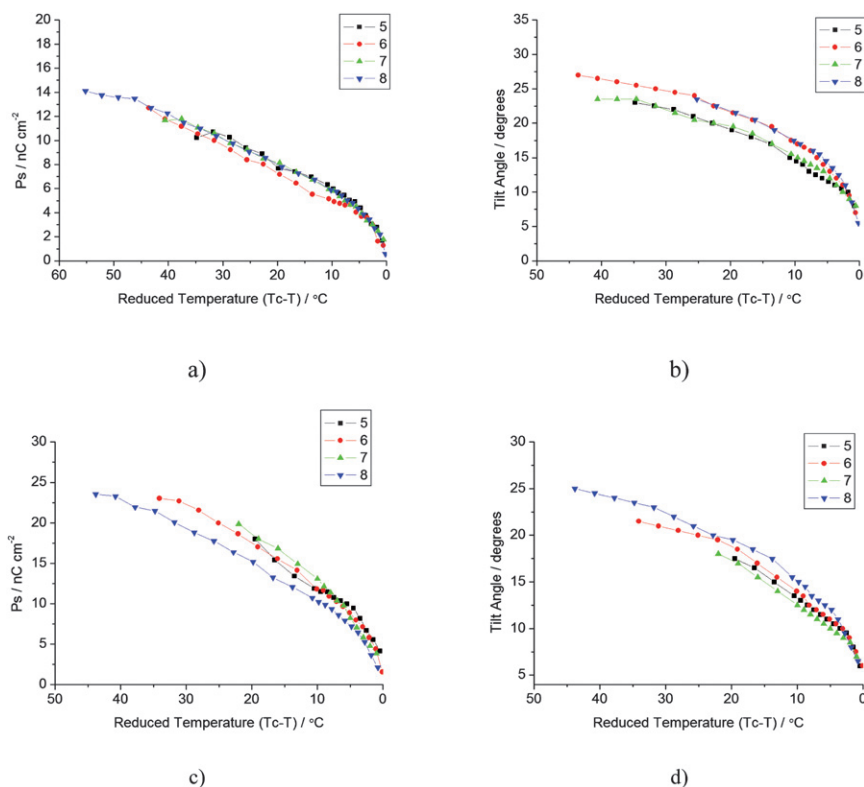
Fig. 5 Spontaneous polarisation and tilt angle measurements for difluoro compounds **5–8** as a function of reduced temperature: (a) and (b) 5 wt% dopant and (c) and (d) 10 wt% dopant.

This journal is © The Royal Society of Chemistry 2010
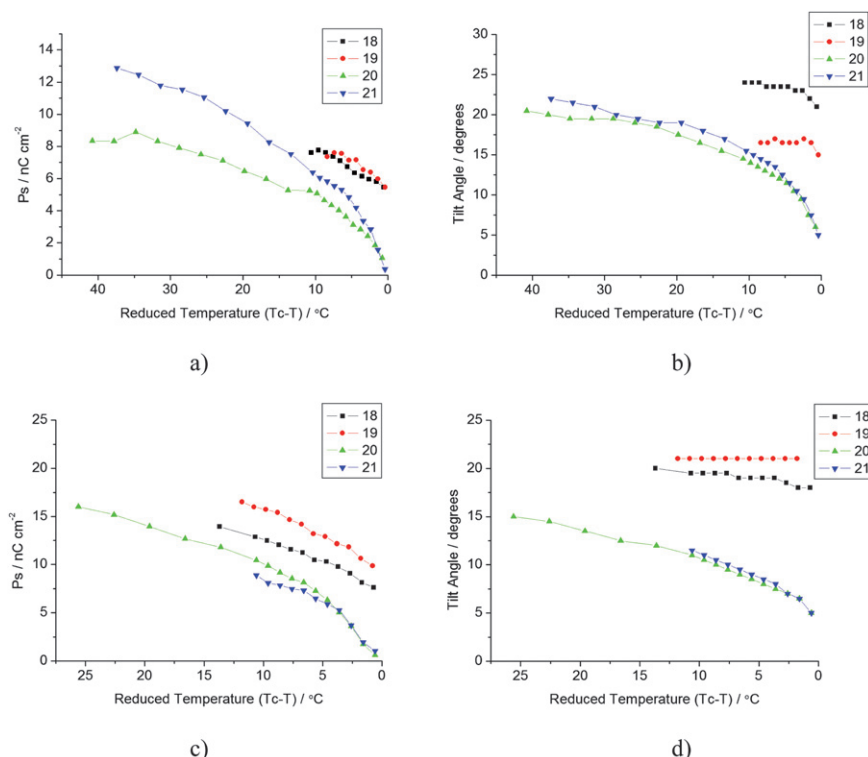
J. Mater. Chem., 2010, **20**, 299–307 | 305

Fig. 6 Spontaneous polarisation and tilt angle measurements for trifluoro compounds **18–21** as a function of reduced temperature: (a) and (b) 5 wt% dopant and (c) and (d) 10 wt% dopant.

compound **8** with dopant **26** Mix1 and Mix2 (with 5 and 10 wt% of dopant, respectively) as function of the reduced temperature and at three voltage levels (10, 20 and 30 V over a cell with a 1.6 μm cell gap). Clearly the response time is much shorter for mixtures containing a larger proportion of the chiral dopant, with response times of below 50 μs at reduced temperatures of up to 30 °C. Obviously the higher the applied field the faster the response, in combination with a high proportion of the dopant response times of less than 10 μs can be achieved.

It was found that the difluoro compounds exhibited good bistability and it was possible to examine these using applied current pulses to calculate the τ–V_{min} curves.[15] These results were in strong agreement with the observed switching times which were determined by applying an ac field of equivalent voltage to the cell at a frequency of 50 Hz. It is clear from the results obtained that there is a significant increase in switching speed

when the voltage is doubled from 10 V to 20 V but there is only minimal difference between the 20 and 30 V measurements. Unfortunately, these compounds tended to exhibit a large number of chevron defects in the cell upon the transition from the smectic A to smectic C phase. This behaviour is associated to the layer shrinkage that occurs as the molecules begin to tilt.

4. Conclusions

The materials reported in this article give a multifaceted approach to the development of liquid crystal display device materials research. The greater the number of fluoro substituents (2–4) located on the *p*-terphenyl core unit the more likely it was found that the material would be nematogenic. The greater the number of fluoro substituents the larger the value of the negative dielectric anisotropy, and the lower the threshold voltage for switching in homeotropically aligned cells. Thus these materials are of interest in vertically aligned nematic liquid crystal display (VAN-LCD) devices. Conversely the fewer the number of fluoro substituents the more likely smectic phases were to be found. For such materials possessing longer aliphatic chains resulted in the stabilisation of smectic C phases, such that the materials exhibit nematic, smectic A and smectic C phases, which is an ideal phase sequence for materials of practical interest as host systems in surface stabilised ferroelectric liquid crystal display (SSFLCD) devices. The incorporation of the chiral dopant BE8OF2N into mixtures with the difluoro-substituted hosts resulted in materials with sub-fifty microsecond response times. Overall this work demonstrates that materials can be developed in tandem for uses in different and diverse LCDs.
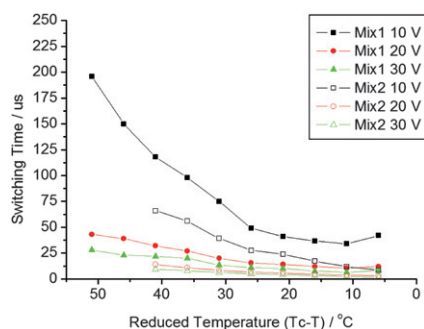

Fig. 7 Switching times for the ferroelectric phase of compound **8** in a 1.6 μm planar aligned cell.

Notes and references

1 J. H. Souk, *Keynote Lecture 2*, 22nd International Liquid Crystal Conference, June 29–July 4, 2008, Jeju, Korea.
2 S. H. Lee, H. Y. Kim, I. C. Park and W. G. Lee, *IEICE Trans. Electron.*, 1998, **E81-C**, 1681–1684.
3 R. Eidenschink, G. Haas, M. Romer and B. S. Scheuble, *Angew. Chem.*, 1984, **96**, 151–160.
4 G. W. Gray, M. Hird, D. Lacey and K. J. Toyne, *J. Chem. Soc., Perkin Trans. 2*, 1989, 2041–2053.
5 M. Hird, J. W. Goodby and K. J. Toyne, Liquid crystal materials, devices and flat panel displays, *Proc. SPIE–Int. Soc. Opt. Eng.*, 2000, **3955**, 15–23.
6 N. Collings, W. A. Crossland, P. J. Ayliffe, D. G. Vass and I. Underwood, *Appl. Opt.*, 1989, **28**, 4740–4747; S. T. Lagerwall, *Liq. Cryst. Today*, 1993, **3**, 1–4; N. A. Clark, C. Crandall, M. A. Handschy, M. R. Meadows, R. M. Malzbender, C. Park and J. Z. Xue, *Ferroelectrics*, 2000, **246**, 97; M. J. O'Callaghan, R. Ferguson, R. Vohra, W. Thurmes, A. W. Harant, C. S. Pecinovsky, Y. Q. Zhang, S. Yang, M. O'Neill and M. A. Handschy, *J. Soc. Inf. Disp.*, 2009, **17**, 369–375.
7 J. W. Goodby, I. M. Saez, S. J. Cowling, V. Görtz, M. Draper, A. W. Hall, S. Sia, G. Cosquer, S.-E. Lee and E. P. Raynes, *Angew. Chem., Int. Ed.*, 2008, **47**, 2754–2787.
8 F. A. Perennes and W. A. Crossland, *Opt. Eng.*, 1997, **36**, 2294–2301.
9 J. W. Goodby, K. J. Toyne, M. Hird, P. Styring, R. A. Lewis, A. Beer, C. C. Dong, M. E. Glendenning, J. C. Jones, K. P. Lymer, A. J. Slaney, V. Minter and L. K. M. Chan, Liquid crystal materials, devices and flat panel displays, *Proc. SPIE–Int. Soc. Opt. Eng.*, 2000, **3955**, 2–14.
10 A. Petrenko and J. W. Goodby, *J. Mater. Chem.*, 2007, **17**, 766–782.
11 M. E. Glendenning, J. W. Goodby, M. Hird and K. J. Toyne, *J. Chem. Soc., Perkin Trans. 2*, 1999, 481–491.
12 G. W. Gray and J. W. Goodby, *Smectic Liquid Crystals—Textures and Structures*, Leonard Hill, Glasgow and London, 1984, 220 p., ISBN 0-249-44168-3.
13 G. W. Gray, M. Hird, D. Lacey and K. J. Toyne, *J. Chem. Soc., Perkin Trans. 2*, 1989, 2041–2053.
14 W. Maier and G. Meier, *Z. Naturforsch., A: Astrophys. Phys. Phys. Chem.*, 1961, **16**, 262–267.
15 J. C. Jones, M. J. Towler and J. R. Hughes, *Displays*, 1993, **14**, 86–90.